STScI | SPACE TELESCOPE SCIENCE INSTITUTE

Instrument Science Report ACS 2017-02

Updated MDRIZTAB Parameters for ACS/WFC

S.L. Hoffmann, R.J. Avila

March 6, 2017
UPDATED: November 27, 2018

Abstract

The Mikulski Archive for Space Telescopes (MAST) pipeline performs geometric distortion corrections, associated image combinations, and cosmic ray rejections with `AstroDrizzle`*. The MDRIZTAB reference table contains a list of relevant parameters that controls this program. This document details our photometric analysis of Advanced Camera for Surveys Wide Field Channel (ACS/WFC) data processed by* `AstroDrizzle`*. Based on this analysis, we update the MDRIZTAB table to improve the quality of the drizzled products delivered by MAST.* ***An update was added November 2018 that explains changes to MDRIZTAB caused by redefining the ACS/WFC data quality flags.***

Introduction

The Mikulski Archive for Space Telescopes (MAST) pipeline offers users easy access to HST observations calibrated and analyzed with the most up-to-date reference files. As part of the regular operation, MAST carries out `AstroDrizzle` processing on relevant observations and supplies FITS images with a DRZ or DRC extension. `AstroDrizzle` is the part of the `DrizzlePac` package that applies the geometric distortion correction to the pixels, combines dithered data, and identifies and masks cosmic rays (Fruchter et al., 2010; Gonzaga et al., 2012).

The MDRIZTAB reference table contains all the parameters used by `AstroDrizzle` when it is called by MAST. The current MDRIZTAB file for the Advanced Camera for Surveys (ACS) Wide Field Channel (WFC) (specifically, ub21537aj_mdz.fits) was created in July 2004, and the last update was in November 2005. MDRIZTAB was created for `MultiDrizzle`, the predecessor of `AstroDrizzle`, hence the "M" in MDRIZTAB. MAST fully implemented `AstroDrizzle` in June 2012, and the similarity in parameter names and functionality enabled continuous use of this reference table.

However, last year during a calculation of the ACS/WFC zeropoints, Bohlin (2016) discovered discrepancies between aperture photometry measurements before and after processing with `AstroDrizzle`, particularly for sources near the saturation limit of ACS/WFC, and included details in his § Appendix A. Mack et al. (2007) previously encountered this problem and proposed a partial solution, but their suggestions were never reflected in the MDRIZTAB.

In an effort to improve the quality of the images for the community directly from the pipeline, we optimized the `AstroDrizzle` parameters in the MDRIZTAB reference table. In this report, we describe the ACS/WFC observations and data reduction in § Observations and Image Processing, the methodology of our aperture photometry in § Photometry, an analysis and interpretation of the photometry in § Analysis, and finally, a summary of the work presented here in the § Conclusion section. **An § UPDATE was added in November 2018 to reflect changes to the ACS/WFC data quality flags.**

Observations and Image Processing

We used two types of ACS/WFC observations in the course of this analysis: the standard stars from Bohlin (2016) and images of the nearby globular cluster NGC 6397.

Standard stars

The nine standard stars utilized here are observed with the WFC1-1K aperture. This is a 1K×1K subarray of the WFC1 CCD and is one of the standard subarrays defined in the ACS Instrument Handbook, although it is now deprecated (Avila et al., 2017). The plate scale of ACS/WFC is $\sim 0\farcs05$/pixel. All Each observation is split into two images of equal exposure time to enable cosmic ray rejection, but there is no dither between the images. Table 1 shows the coordinates, observation date and proposal identification number for all the observed epochs of the standard stars. Additional information about the standard stars can be found in Bohlin (2016) Table 1.

When available, we used filters F435W, F475W, F550M, F555W, F606W, F625W, F775W, F814W and F850LP. In particular, two stars (2M0036+18 and 2M0559−14) are only observed in the three longest wavelength filters due to their low temperature.

We downloaded the FITS FLT images from MAST, which do not have the charge transfer efficiency (CTE) correction applied. Images corrected for CTE (denoted by an FLC extension) are not generated for subarrays, and we do not expect to see any effects on bright standard stars with our relative photometry method. We used the `acsrej` program in the `CALACS` module from AstroConda to generate cosmic ray-rejected CRJ images from the pair

of exposures taken at each visit. This is the same procedure MAST uses to create CRJ images. Then we multiplied the relevant section of the Pixel Area Maps[1] (PAMs) corresponding to the footprint of the WFC1-1K aperture with the CRJ frames so that the CRJ flux values could be compared to the geometric distortion-corrected flux values measured from drizzled images.

We drizzled the FLT images with MDRIZTAB set to True, which automatically sets the `AstroDrizzle` parameters to those contained in the reference file. First we used the current reference file (ub21537aj_mdz.fits), and then we produced modified reference files that contained any changes to the `AstroDrizzle` parameters. In this way, we could test the input parameters while still implementing the MDRIZTAB table.

NGC 6397

NGC 6397 is the second closest globular cluster to Earth and is located in the southern constellation Ara at an R.A. $= 17^h40^m41^s$ and Dec. $= -53°40'25''$. In 2005, a field $5'$ SE from this core position was imaged with the full ACS/WFC aperture as part of Cycle 13 (GO-10424, PI: Richer). Each orbit of the 126 orbit program was divided into two F814W images and one F606W image. Images had a typical exposure time of 750 s with a small dither between them (Richer et al., 2006; Anderson et al., 2008; Richer et al., 2008).

This program was ideal for our `AstroDrizzle` calibration test for several reasons. The outer field of the globular cluster is populous enough to contain a healthy sample size of stars while the spatial separation between sources means that crowding is typically not an issue at the aperture radius we examine in this work. Additionally, these stars cover a wide range of magnitudes, including a significant number of objects at or beyond the saturation limit. Such stars are necessary as Bohlin (2016) found an increased scatter in his photometry of standard stars measured on DRZ images when compared to that measured on CRJ images near the saturation limit. Finally, the repeated observations of this field allowed for large groups of dithered image associations of both F606W and F814W taken during the same visit. The largest associations are 5 images in F606W and 10 in F814W.

We did not require the full set of images in this program as our interest is in using the bright stars as standards to calibrate `AstroDrizzle` and not in creating deep color-magnitude diagrams or finding faint white dwarfs like the original research proposal. All of the images we processed and present in this work are listed in Table 2, along with their exposure time and filter.

As before, we downloaded the ACS/WFC images from MAST and generated three sets of data products: PAM-corrected FLC images, images drizzled by `AstroDrizzle` with the current MDRIZTAB option set to True, and a final set of drizzled images using an updated MDRIZTAB table that contained changed parameters.

Photometry

We performed aperture photometry on the drizzled images using the `photutils` software (Bradley et al., 2016). We identified stars with the `daofind` routine which is an implemen-

[1] http://www.stsci.edu/hst/acs/analysis/PAMS

tation of the FIND algorithm from the commonly used DAOPHOT (Stetson, 1987). We ran daofind with a full width at half max (FWHM) input of 2.5 pixels and a detection threshold of 10σ.

For the Bohlin (2016) standard stars, we were only interested in the brightest object in the middle of the image and ignored any other detected source. We then measured the counts in each image with circular apertures using the CircularAperture tool from photutils. We used apertures of 20 pixels (or $1''$) to match the photometry of Bohlin (2016). We also calculated the sky background using the CircularAnnulus tool with inner and outer radii of 25 and 35 pixels in order to subtract the background. We applied this same photometry method to the drizzled DRZ images and the PAM-corrected CRJ images to produce equivalent measurements that we compare in the next section.

In NGC 6397, a threshold of 10σ generated a list of $\sim 10^4$ sources with the exception of instances where we processed only one image (N=1). In this case, AstroDrizzle could not perform cosmic ray rejection, and this increased the number of sources to $\sim 3.2 \times 10^4$. We detected the source positions in the DRC images, and then used the geometric distortion information in the header to map those positions to the FLC images with the pixtopix tool from the DrizzlePac package. This ensured that we performed the aperture photometry on the same source in both images even though those sources are at different image positions in the FLC and DRC. We followed a procedure similar to that for the standard stars with respect to the aperture photometry, however the field is too crowded to use a large radius without contamination from spatially adjacent sources. Therefore, we reduced the aperture radius to 5 pixels and the background inner and outer radius values to 10 and 20 pixels, respectively.

Finally, we want to note that the photometry presented in this work is made with the purpose of optimizing AstroDrizzle parameters and only the improvement in the relative measurements are of interest here. As such, we do not need to measure or apply additional aperture corrections or zeropoints when calculating a direct comparison with the same sources, apertures and background annuli.

Analysis

With photometry data produced as detailed in the previous section, we compared the standard star photometry from the CRJ and DRZ generated from the AstroDrizzle parameters in the current MDRIZTAB reference table and recreated the figure from Bohlin (2016), shown here in Figure 1. Approximately 36% of the standard star DRZ/CRJ measurements deviate from unity greater than 1%. The same behavior is found independently for each filter (Figure 2).

The points scatter largely downward (< 1.0) which by our convention means that the DRZ flux value is smaller than the CRJ. We can conclude that something in the AstroDrizzle process is removing flux from the stars. A discussion of the likely cause from Bohlin (2016) advocates a change of the AstroDrizzle parameter *driz_cr_scale* from (1.2, 0.7) to (1.5, 1.2). The larger values relax how strictly AstroDrizzle identifies cosmic rays, which prevents the cores of stars from being incorrectly flagged and removed (see Gonzaga et al. (2012) § 4.2.7 for more detail). Additionally, we determined in this work that AstroDrizzle masks a

significant amount of the flux of the source because it is flagged in the data quality (DQ) extension for meeting or exceeding the full well saturation value, which for ACS/WFC is $\sim 8 \times 10^4\, e^-$ (Gilliland, 2004). We therefore change *driz_sep_bits* and *final_bits* to allow this flag by adding 256. We make no changes for the A-to-D saturation because the majority of the ACS/WFC images are observed with a gain of two and thus do not reach this saturation limit. All the proposed changes to the `AstroDrizzle` parameters contained in the MDRIZTAB reference table can be found in Table 3.

We implemented these changes and repeated the photometry comparison and discovered that, indeed, the scatter was reduced, see Figure 3 compared to Figures 1 & 2. Charge is not lost but moves along the columns for saturated pixels. We therefore enable accurate aperture photometry by ignoring the saturation flag and retaining these pixels in the `AstroDrizzle` processing. With the new parameters, only $\sim 16\%$ of the observations have an offset between the CRJ and DRZ photometry measurements greater than 1%. We investigated the remaining discrepancies and discovered that one of the epochs happened to position the star on a hot pixel that was correctly flagged and masked by `AstroDrizzle`. We would not expect the CRJ and DRZ photometry to match in this particular situation due to the masked hot pixel. In any case, most modern observing programs follow recommended procedures and dither between images in order to remove the effects of such detector imperfections.

Given that, we used images of NGC 6397 to verify the `AstroDrizzle` parameters for dithered data. The MDRIZTAB reference table already contained options for associations with 1, 2, and 6 images. We added the 4 image association (N=4) because it is one of the most commonly generated data sets due to the predefined box dither pattern provided for ACS/WFC. The simplest case is N=1 because with a single image no dither is possible and therefore no cosmic ray rejection or other calibration based on multiple images can be performed. Starting here, we find that the best procedure is to allow all the pixels to be utilized by `AstroDrizzle` regardless of the flags in the DQ array (*final_bits*= 65535). Figure 4 shows the photometry comparisons for the current and new `AstroDrizzle` parameters. We measured the standard deviation of each sample, selecting stars with peak values of $2 \times 10^4 - 10 \times 10^4\, e^-$, and found that the scatter is reduced by 92% with the new parameters. Figure 5 displays the same information in histogram form to illustrate that the most populated bin, which contains a DRC/FLC value of 1.0, increases by thousands of sources due to the elimination of an asymmetrical feature in the current photometry.

While this is an obvious improvement, a diffuse cloud of points remains at the brightest end in the new photometry of Figure 4 and required investigation. Figure 6 shows a portion of an image of the NGC 6397 field and the DRC/FLC ratio of the photometry. We selected both well-behaved points near unity (highlighted in blue) and offset points (red) and visually examined the corresponding sources on the image. We found that the red, scattered points belong to the brightest stars with extended saturation trails, or sources contaminated by image artifacts. The blue, well-behaved points fall on isolated stars with no major trails. We do not anticipate accurate photometry measurements of highly saturated sources with a 5 pixel aperture, and therefore we conclude that this scattered cloud of points is an expected consequence of our photometry and do not address it further.

We do want to remind users here that the full well depth is not an absolute cutoff point. Figure 4 from Gilliland (2004) demonstrates that there is a spatial dependency across the detector with variations of 10% which is not corrected for or addressed in this work. We

attribute the small trend that offsets the brightest stars from unity to these saturation effects (see the upturn in the bottom panel of Figure 4 in points greater than $8 \times 10^4\, e^-$). Additionally, such a small discrepancy does not negate the dramatic improvement of the photometry achieved here, especially in light of the fact that no object of interest in a science program should be observed this far above the saturation limit.

We repeated this analysis on the associations containing 2, 4 and 6 images. We do not include the redundant plots with similar results to Figures 4-6, but note that we saw a large statistical improvement in each trial as shown in Table 4. We also examined the *combine_type* parameter to determine if the images should be combined with the minmed or median option. The minmed option is more conservative than median because it works by replacing median values significantly above a good pixel value with a lower value. We found an improvement in the photometry when using median for the N=4 case, but acknowledge that the median is less robust in areas with less image depth, such as at the edges of the aperture and on the chip gaps. We decided that the improvement in measurement accuracy and precision across the image made the choice of median worthwhile, but users should be advised that the median in these limited areas is not ideal and will need reprocessing with minmed if an object of interest happens to fall on these parts of the image. The combination of parameters that produce the most accurate and precise aperture photometry is in Table 3.

Conclusion

As we have shown in this work, we improved the photometry measurements of the MAST generated drizzled images with select changes to a small number of the `AstroDrizzle` parameters (Table 3) set by the MDRIZTAB reference table. Additionally, we now include an optimization for associations of 4 images, one of the most popular dither patterns. While it is still recommended that each user find and implement the best `AstroDrizzle` configuration for their specific program, this improved MDRIZTAB reference table will increase the utility and reliability of the drizzled images and provide users with a higher quality product directly from the archive.

Acknowledgements

This research made use of Astropy, a community-developed core Python package for Astronomy (Astropy Collaboration et al., 2013), as well as the Python-based data interface Glueviz, which can be found at http://glueviz.org/. We thank Jennifer Mack for her helpful comments and sharing her `AstroDrizzle` expertise.

References

Anderson, J., King, I. R., Richer, H. B., et al. 2008, AJ, 135, 2114

Astropy Collaboration, Robitaille, T. P., Tollerud, E. J., et al. 2013, A&A, 558, A33

Avila, R., et al. 2017, Advanced Camera for Surveys Instrument Handbook for Cycle 25 v. 16.0 (STScI)

Bohlin, R. C. 2016, AJ, 152, 60

Borncamp, D., Grogin, N., Bourque, M., & Ogaz, S. 2017, Pixel History for Advanced Camera for Surveys Wide Field Channel, Tech. rep., STScI

Bradley, L., Sipocz, B., Robitaille, T., et al. 2016, astropy/photutils: v0.3, Zenodo, doi:10.5281/zenodo.164986. `https://doi.org/10.5281/zenodo.164986`

Fruchter, A. S., Hack, W., Dencheva, N., Droettboom, M., & Greenfield, P. 2010, in 2010 Space Telescope Science Institute Calibration Workshop, p. 382-387, 382–387

Gilliland, R. L. 2004, ACS CCD Gains, Full Well Depths, and Linearity up to and Beyond Saturation, Tech. rep., STScI

Gonzaga, S., Hack, W., Fruchter, A., & Mack, J. 2012, The DrizzlePac Handbook (STScI)

Mack, J., Gilliland, R. L., Anderson, J., & Sirianni, M. 2007, WFC Zeropoints at -81C, Tech. rep., STScI

Richer, H. B., Anderson, J., Brewer, J., et al. 2006, Science, 313, 936

Richer, H. B., Dotter, A., Hurley, J., et al. 2008, AJ, 135, 2141

Stetson, P. B. 1987, PASP, 99, 191

Table 1. Standard star observations

Name	α J2000	δ J2000	Date	Prop ID	Name	α J2000	δ J2000	Date	Prop ID
G191B2B	76.377	52.831	2003-11-07	10054	BD+17D4708	332.882	18.093	2009-09-21	11889
			2005-02-27	10374				2011-10-24	12737
			2011-02-13	12392				2013-09-04	13162
			2011-11-10	12737					
			2013-03-01	13162	P330E	247.891	30.146	2006-01-18	10374
			2014-09-19	13599				2009-08-07	11889
			2014-11-03	13962				2011-07-14	12392
			2015-11-20	14405					
					KF06T2	269.658	66.781	2009-08-09	11889
GD153	194.259	22.030	2003-11-12	10054				2011-03-04	12392
			2005-04-20	10374				2012-03-20	12737
			2007-01-16	11054					
			2009-08-09	11889	VB8	253.895	-8.396	2004-02-08	10056
			2012-04-28	12737				2005-05-11	10374
			2013-05-20	13162				2009-08-09	11889
			2014-06-07	13599				2013-03-11	13162
			2015-05-01	13962					
			2016-03-05	14405	2M0036+18	9.067	18.353	2005-01-03	10374
								2006-06-10	10740
GD71	88.115	15.886	2003-11-03	10054					
			2006-09-11	10740	2M0559-14	89.830	-14.080	2003-09-15	10056
			2011-02-22	12392				2005-04-02	10374
			2011-10-23	12737					
			2012-11-01	13162					
			2014-08-11	13599					
			2015-02-01	13962					
			2016-02-22	14405					

Table 2. NGC 6397 observations

Rootname	Filter	Exp. Time (seconds)	Rootname	Filter	Exp. Time (seconds)
j97113nqq	F606W	769.0	j97101bbq	F814W	616.0
j97113p9q	F606W	769.0	j97101bfq	F814W	649.0
j97112g6q	F606W	769.0	j97101bhq	F814W	804.0
j97112gcq	F606W	769.0	j97101blq	F814W	649.0
j97112giq	F606W	769.0	j97101bnq	F814W	804.0
j97112goq	F606W	769.0	j97101brq	F814W	649.0

Table 3. MDRIZTAB parameter changes

numimages	driz_sep_bits		combine_type		driz_cr_scale		final_bits	
	Previous	New	Previous	New	Previous	New	Previous	New
N=1	32+64	65535	minmed	INDEF	1.2 0.7	INDEF	32+64	65535
N=2	32+64	32+64+256	minmed	minmed	1.2 0.7	1.5 1.2	32+64	32+64+256
N=4		32+64+256		median		1.5 1.2		32+64+256
N=6	32+64	32+64+256	median	median	1.2 0.7	1.2 0.7	32+64	32+64+256

Note. — The previous values for four images (N=4) are left blank because the N=4 case did not exist in earlier versions of the MDRIZTAB reference file. `AstroDrizzle` defaulted to the two image (N=2) parameters when it processed four images. The value of 65535 is a sum of all the possible flag values and will cause `AstroDrizzle` to disregard all flags.

Table 4. NGC 6397 DRC/FLC photometry comparison results

Num. of Images	Mean		Median		Std. Dev.	
	Previous	New	Previous	New	Previous	New
N=1	0.87	1.00	0.88	1.00	0.14	0.01
N=2	0.82	1.00	0.81	1.00	0.16	0.02
N=4	0.78	1.00	0.76	1.00	0.18	0.02
N=6	0.84	0.99	0.84	1.00	0.16	0.02

Table A. Update of Table 3: MDRIZTAB parameter changes for unstable pixel flag

numimages	driz_sep_bits			final_bits		
	Previous 2005	"New" 2017	Update 2018	Previous 2005	"New" 2017	Update 2018
N=1	32+64	65535	65535	32+64	65535	65535
N=2	32+64	32+64+256	16+64+256	32+64	32+64+256	16+64+256
N=4		32+64+256	16+64+256		32+64+256	16+64+256
N=6	32+64	32+64+256	16+64+256	32+64	32+64+256	16+64+256

Note. — This table contains only the parameters affected by the addition of unstable pixels to the DQ flag definitions. See Table 3 for other MDRIZTAB parameters. The previous values for four images (N=4) are left blank because the N=4 case did not exist in earlier versions of the MDRIZTAB reference file. `AstroDrizzle` defaulted to the two image (N=2) parameters when it processed four images. The value of 65535 is a sum of all the possible flag values and will cause `AstroDrizzle` to disregard all flags.

UPDATE

In early 2017 when this work was published, the data quality (DQ) flag of 32 was included in the *driz_sep_bits* and *final_bits* parameters of MDRIZTAB, which select the pixels `AstroDrizzle` considers valid. The DQ flag 32 was added when MDRIZTAB was first made because 32 marked CTE tails, but the ACS team discarded this definition years before and 32 was long undefined by 2017. The DQ flag 32 was kept for historical reasons in MDRIZTAB since there was no harm in identifying an empty flag for `AstroDrizzle` when processing images.

However, later that year a metric for analyzing ACS/WFC pixels was introduced based on how each pixel behaves over time (Borncamp et al., 2017, ACS ISR 17-05). Pixels are now classified as stable or unstable depending on whether they can be accurately corrected by the dark in the ACS calibration pipeline (stable) or whether their behavior is too variable over time to correct (unstable). The newly defined unstable pixels were assigned to the null flag value of 32 and became a flag that `AstroDrizzle` needs to account for when processing images. This represents a shift away from discarding all pixels classified as "hot". As long as the "hot" pixels are stable, they can be accurately calibrated with the dark, albeit with an increased error compared to their cooler counterparts appropriately recorded in the error array.

A modified MDRIZTAB was submitted to reflect this change. In this version, the 32 flag was removed from *driz_sep_bits* and *final_bits* and replaced by 16, resulting in `AstroDrizzle` using stable "hot" pixels (16) as valid pixels and rejecting unstable pixels (32) as invalid when combining images. These updated MDRIZTAB parameters are listed in Table A.

We encourage readers interested in pixel history and stability to consult Borncamp et al. (2017), which includes an explanation of the changes to MDRIZTAB and the resulting `AstroDrizzle` behavior in Section 4.

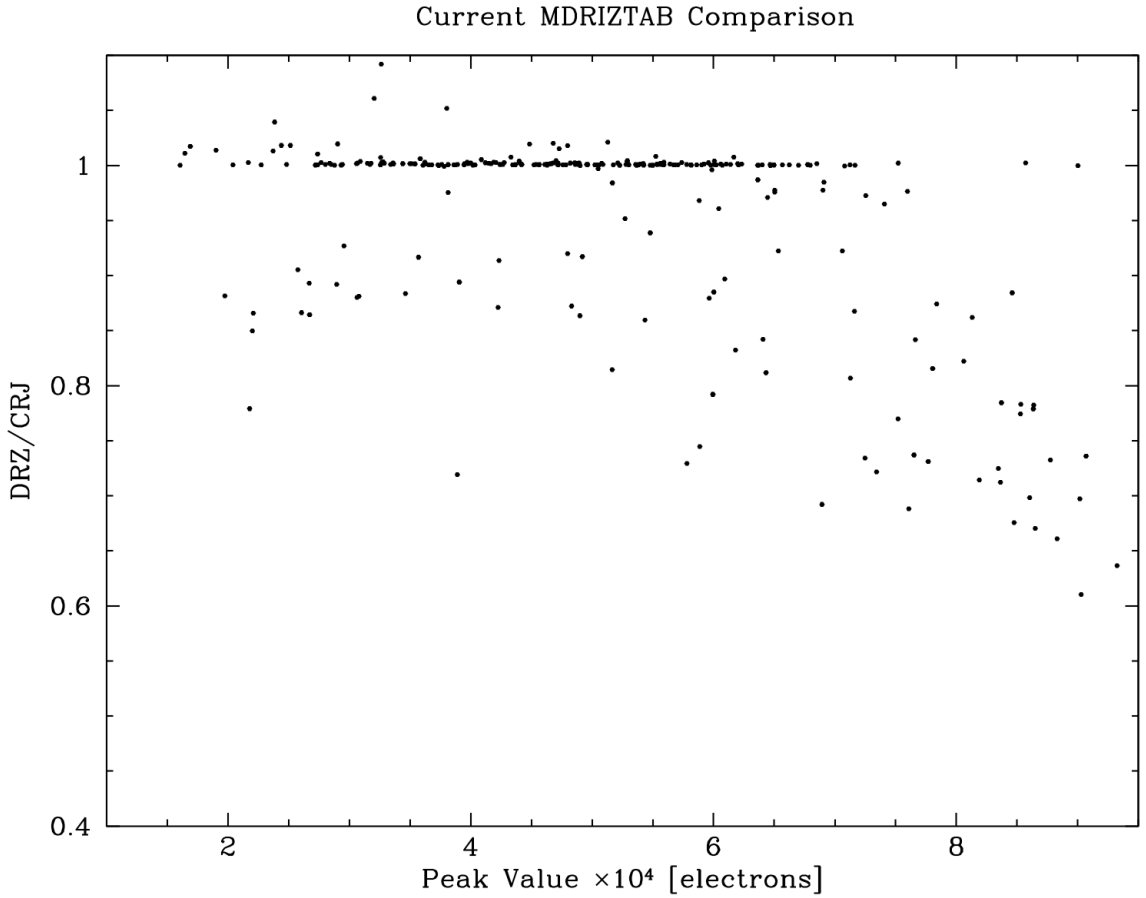

Figure 1 - DRZ/CRJ ratio of standard star aperture photometry as a function of the central pixel value of the source. A significant amount of scatter is seen with 36% of the observations differing from the expected value of one by 1%, preferentially at the brighter end where the sources exceed the full well saturation limit of $\sim 8 \times 10^4\, e^-$.

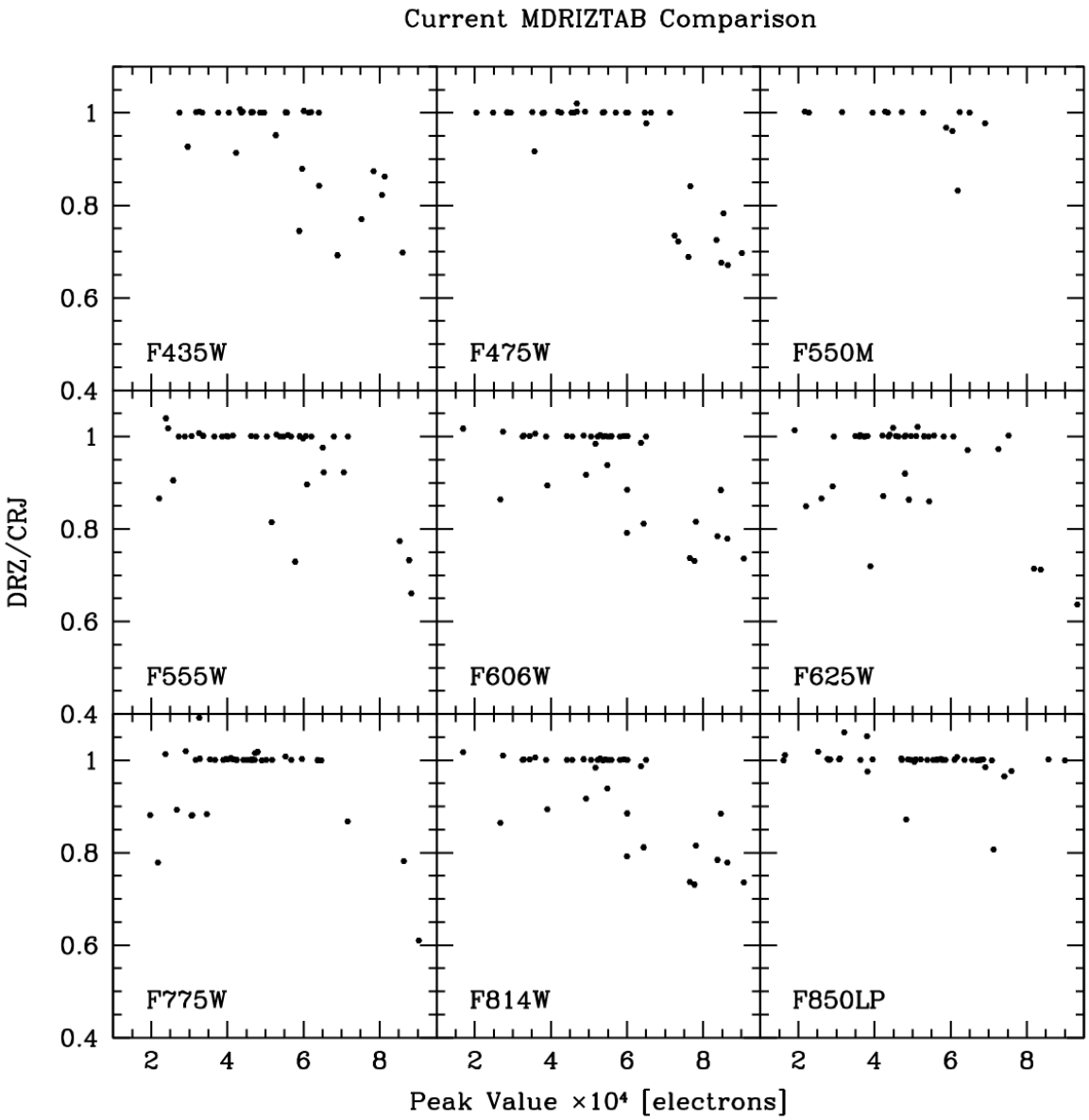

Figure 2 - Same photometry comparison as in Figure 1 but now separated by filter. It is clear that the behavior illustrated in Figure 1 is filter independent.

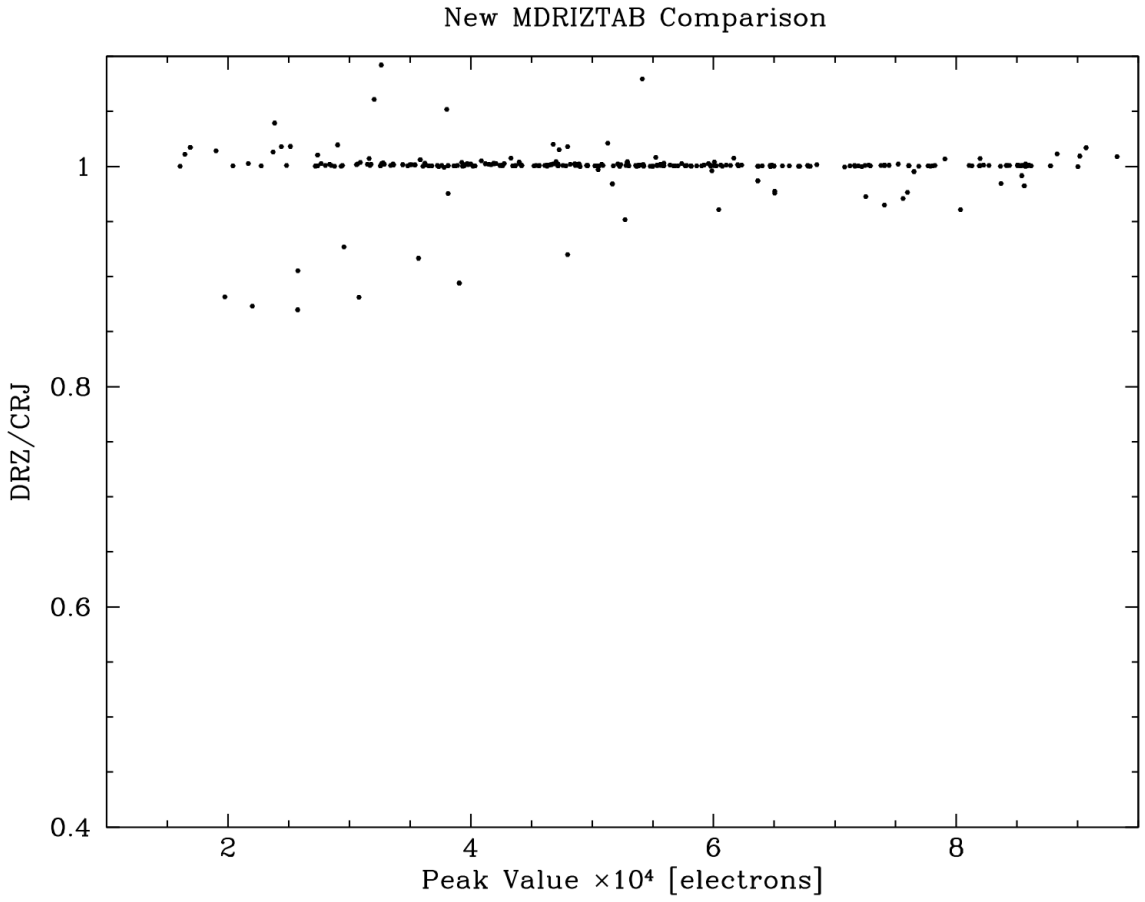

Figure 3 - The photometry comparison of standard stars after MDRIZTAB parameters are changed to optimize `AstroDrizzle` image output. The scatter is much reduced compared to Figure 1, and the few surviving outliers are due to hot pixels that are flagged in the drizzled DRZ but not the CRJ image.

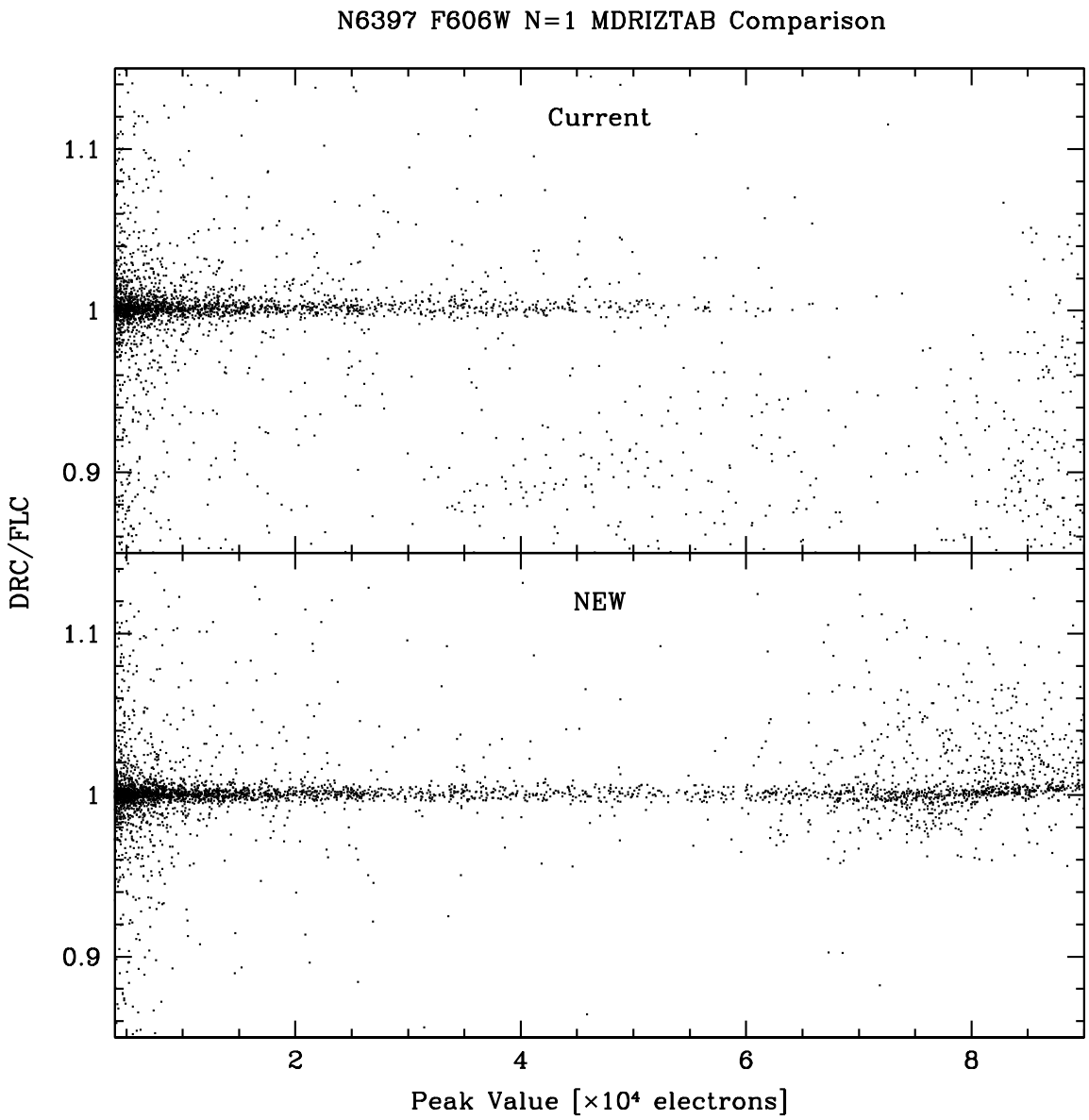

Figure 4 - Shown here is the photometry comparison of an FLC image from MAST and its drizzled DRC counterpart for both the current (top panel) and the new MDRIZTAB parameters (bottom panel) of a single F606W image (N=1) of the globular cluster NGC 6397. Points at the bright end located below the axis of the plot in the top panel are well behaved with the new parameters.

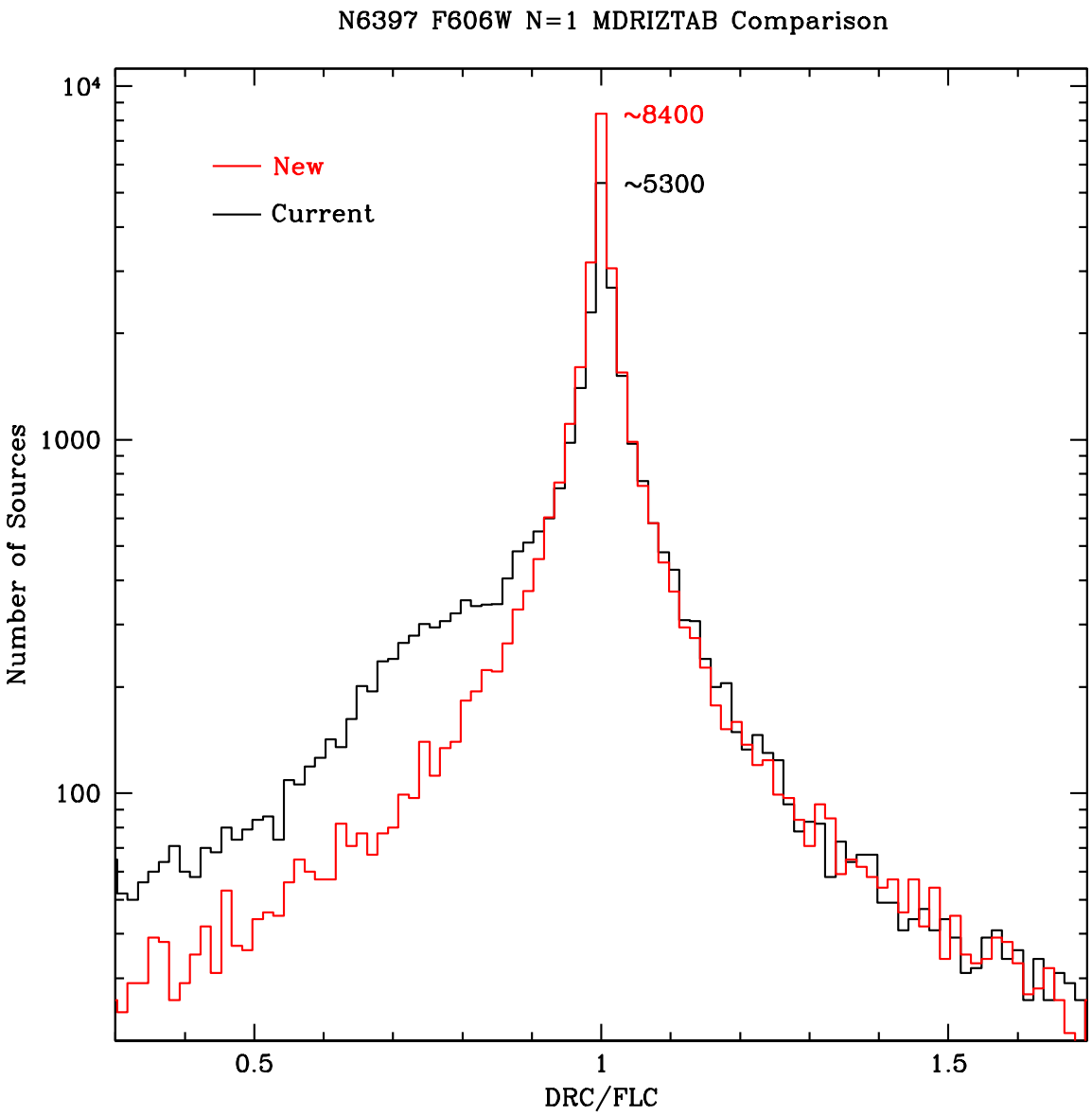

Figure 5 - A log-scale histogram of the same data presented in Figure 4. The current parameters are shown in black, and the new in red. The feature on the left side of the histogram seen in the current parameters (black line) disappears, and the new parameters form a symmetric distribution (red line). The number of points contained in the peak bin is displayed to highlight the significant change between the two distributions.

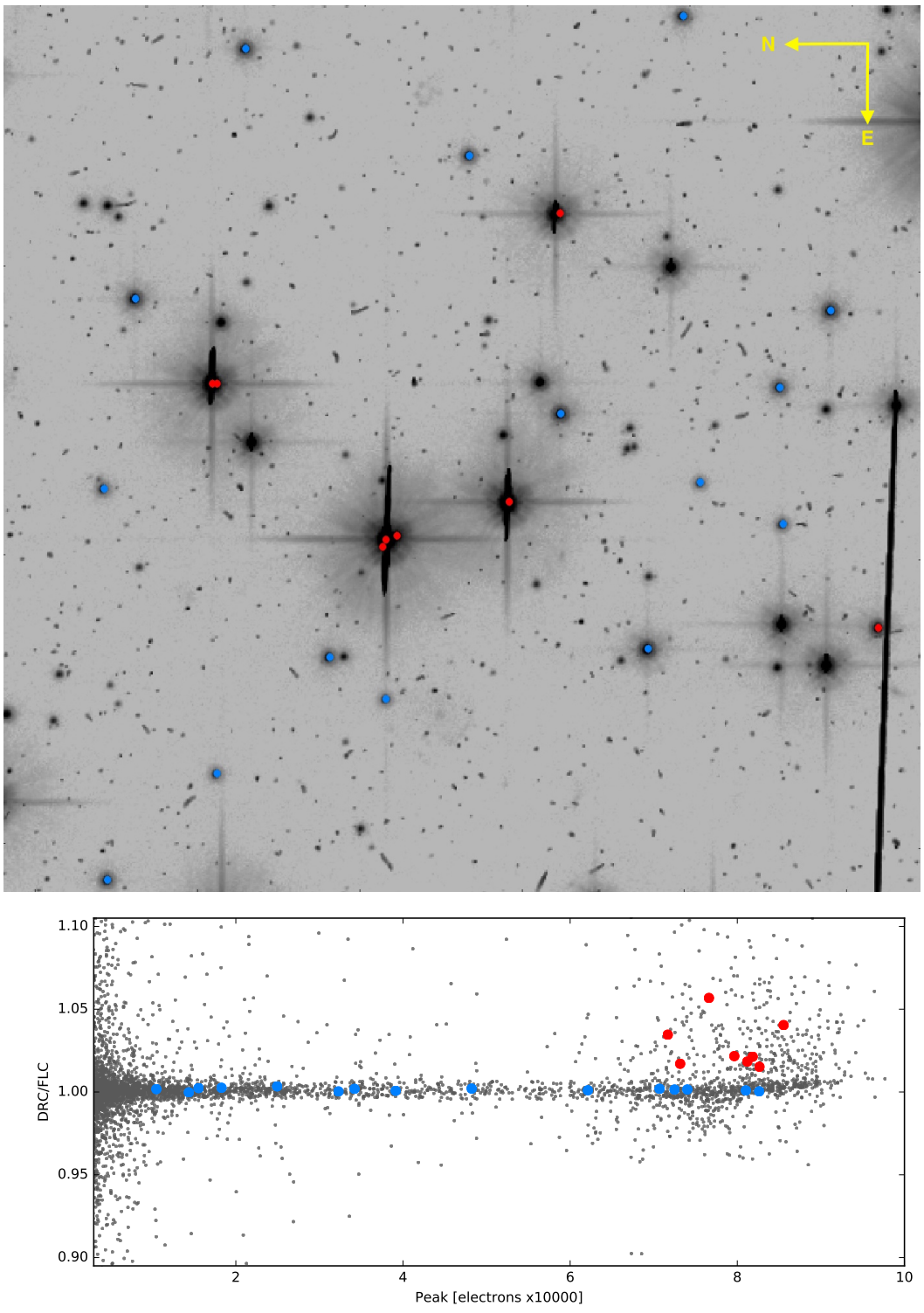

Figure 6 - A small region ($27'' \times 27''$) of an F606W N=1 dithered ACS/WFC NGC 6397 field is displayed above a reproduction of the DRC and FLC photometry comparison in Figure 4. The larger, blue points are well-behaved in the photometry and map to isolated stars without large saturation trails. The red points identify the scattered stars as heavily saturated or otherwise contaminated by image artifacts.